ISSN: 0067-2904

Electrochemical Study of Inhibition for Low Carbon Steel Corrosion in the Saline Medium through a Novel Polymer-metal oxides Nanocomposite

Zainab Hussain*, Khulood A. Saleh
Department of Chemistry, College of Science, University of Baghdad, Baghdad, Iraq.

Received: 4/10/2023 Accepted: 16/7/2024 Published: 30/4/2025

Abstract

In this work, new conductive polymer (4900 µs.cm-1) poly 6-((4-sulfamoylphenyl)carbamoyl)cyclohex-3-ene-1-carboxylic acid (PSCC) was prepared on a Low Carbon Steel (L.C.S) surface by an electrochemical polymerization process for its monomer 6-((4-sulfamoylphenyl)carbamoyl)cyclohex-3-ene-1-carboxylic acid (SCC) to study the effect of this polymer against corrosion of the L.C.S in salt environment (3.5% wt NaCl) at four temperatures; 25, 35, 45, and 55 ^{o}C. Two types of nanometal oxides, ZrO_2 and ZnO, were applied as additives to the polymer (PSCC) to enhance the ability of this polymer on corrosion protection L.C.S alloy. Potentiostatic polarization tests evaluated the corrosion performance of the coatings. Atomic Force Microscopy (AFM) and Scanning Electron Microscopy (SEM) study the coatings' topography and morphology of the surfaces. The study determined and analyzed the kinetic and thermodynamic parameters associated with the activation energy required for the corrosion reaction to occur. The results indicate that the prepared polymer effectively reduced the corrosion of L.C.S, and the addition of nanometal oxides further enhanced the polymer's performance in protecting the alloy from corrosion.

Keywords Electropolymerization, Conducting polymers, nanocomposite, Tafel, L.C.S.

دراسة كهروكيميائية لتثبيط تأكل الفولاذ منخفض الكربون في الوسط الملحي من خلال استخدام متراكبات نانوية لاكاسيد فلزية مع بوليمرات جديدة

زينب حسين*, خلود عبد صالح
قسم الكيمياء, كلية العلوم, جامعة بغداد. بغداد, العراق

الخلاصة

في هذه الدراسة, تم استخدام تقنية البلمرة الكهربائية في بلمرة المونومر 6-((4- sulfamoylphenyl)carbamoyl)cyclohex-3-ene-1-carboxylic acid (SCC) كهربائيا على سطح الفولاذ منخفض الكربون لتحضير البوليمر الموصل poly 6-((4-sulfamoylphenyl)carbamoyl)cyclohex-3-ene-1-carboxylic acid (PSCC) و الذي تبلغ توصيليته (4900 مايكروسيمنز . سم $^{-1}$) والذي يعمل كطلاء يحمي سطح سبيكة الفولاذ منخفض الكربون من التأكل بفعل الوسط الملحي (3.5% كلوريد الصوديوم) عند درجات حرارة 25, 35, 45, و 55م . تم استخدام اثنين من الاكاسيد النانوية كمضافات للبوليمر وهي (اوكسيد الزركونيوم و اوكسيد الزنك) لتعزيز قدرة البوليمرعلى

*Email: Zainab_alaa@gmail.com

حماية السبيكة من التآكل. تم استخدام جهاز potentiostt لمعرفة مدى كفاءة هذه الطلاءات البوليمرية في حماية السبيكة من التآكل. كما تم استخدام جهاز حيود الاشعة السينية , مجهر القوة الذرية, والمجهر الماسح الالكتروني لدراسة مكونات الاطوار, مورفولوجية السطح وتوزيع العناصر. تم حساب ومناقشة معلمات التنشيط الحركية والثرموداينمكية المرتبطة بطاقة التنشيط اللازمة لحدوث تفاعل التآكل. تشير النتائج إلى أن البوليمر المحضر قلل بشكل فعال من تآكلL.C.S ، كما أن إضافة أكاسيد المعادن النانوية عززت أداء البوليمر في حماية السبيكة من التآكل.

.**Introduction**

Corrosion of metals is a major global issue [1] as metals are thermodynamically more stable when chemically combined in compounds rather than in their elemental metallic form [2]. Since most metals exist in the form of oxides, while extracted in a free state, a lot of energy is provided to them. This energy allows them to return to their combined condition when exposed to the outside environment, such as moisture, oxygen, etc. For example, when iron is exposed to the environment, it undergoes corrosion, forming hydrated ferrous oxide, which manifests as a brown substance. This indicates that corrosion is a process that contradicts the extraction of minerals [3]. (Eq. (1)).

$$\text{Metal} \underset{\text{Metal Extraction}}{\overset{\text{Corrosion}}{\rightleftharpoons}} \text{Metal Oxides + Energy} \quad .....(1)$$

Carbon steel is one of the important iron alloys, as one of its most prominent components is iron and carbon. It has broad use in numerous industries and is the most flexible, economical, and commonly utilized engineering material [4]. Large tonnages are used in pipelines, mining, construction, transportation, chemical processing, nuclear and fossil fuel power plants, marine applications, and metal processing machines. However, carbon steel exhibits relatively poor corrosion resistance, leading to numerous corrosion-related issues in associated industries [5].

Various methods have been used to protect the precious metals from corrosion. The use of conductive polymers as a coating is of great scientific importance because old techniques and methods like coatings using paints are not valid. After all, they contain toxic and hazardous constituents, while conducting polymers do not contain toxic and hazardous ones for the environment. In addition, Conducting Polymers (CPs) provide both physical and electronic barrier effects and electromagnetic interference (EMI) shielding, which enhances the protection behaviour [6], compared to traditional coatings that only provide physical barriers against corrosive environments [7].

To create CPs, oxidative electrochemical techniques or electropolymerization are typically used [8] because they offer multiple advantages, such as (i) making it simple to functionalize conductive surfaces precisely; (ii) allowing for the formation of films with good reproducibility and controlled thickness; and (iii) producing densely packed layers that make the process of electron hopping between macroscopic molecules easier[9].

Likely the most common approach to providing corrosion protection through polymer coatings is by creating a barrier that isolates the metal surface from the corrosive environment. The polymeric material must provide correct barrier qualities and maintain adhesion in water and corrosive substances like Fe_2O_3 to isolate surfaces effectively [10].

In polymeric coatings, nanoparticles are utilized to provide coatings with strong adhesion, good durability, and high surface mechanical abrasion resistance that are in great demand. [11].

The term "polymer nanocomposite" refers to a multi-constituent substance, one of whose major constituents is a polymer or its mixture and whose minor constituent has a nanoscale dimension. Because of their nanoscale and filler dispersion, which improve their properties and give them a special and unique quality for use in a variety of applications, one of which is the inhibition of metal corrosion, polymer nanocomposites are the best substitute for conventional fillers of polymers [12-16].

This study developed a new conductive polymer coating for protecting L.C.S. alloys against corrosion via an electropolymerization deposition method. Nano oxides (ZrO_2 and ZnO) were added to the coating solution to enhance other performance characteristics, including adhesion, thermal stability, mechanical strength, hydrophobic properties, and magnetostatic shielding.

2. Experimental Part

2.1 Sample preparation

L.C.S (CK37) sheet was used to make thin disks with thicknesses and diameters of 15 mm and 25 mm, respectively. The chemical composition of the steel was determined using x-ray fluorescence spectroscopy. It was found to contain C (0.1%), Cu (0.022%), Mn (0.39%), Si (0.005%), and Fe (99.3%), along with various other elements totaling 0.18%. Carbon steel disks were mechanically polished with varied SiC paper 180, 220, 400, 1200, 2000, and 2500 grit, followed by washing in distilled water and ethanol, drying in warm and dry airflow, and storage in a desiccator. Figure 1 shows the L.C.S disks before and after polishing.

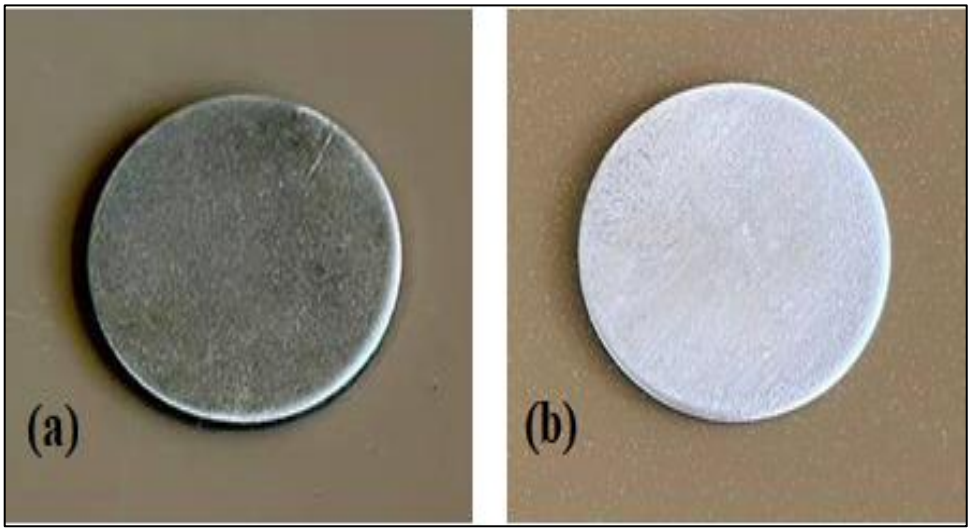

Figure 1: The L.C.S discs (a) before the Polishing (b) after the polishing.

2.2 Electropolymerization Technique

The monomer 6-((4-sulfamoylphenyl)carbamoyl)cyclohex-3-ene-1-carboxylic acid (SCC) was electropolymerized on the surface of L.C.S alloy using a DC power source and two electrodes: The counter electrode (CE) was a stainless steel plate and the working electrode (WE), which is an L.C.S. disc. Three drops of 95% H_2SO_4 were added to 100 milliliters of D.W. containing 0.1 grams (0.003 M) of SCC monomer as the coating solution for electropolymerization. After applying an approximate voltage of 1.5 V for 60 minutes at ambient temperature, a heat gun was used to dry the coated electrode. In addition, To increase polymer films' resistance to corrosion, ZrO_2 and ZnO nanoscale metal oxides were added at a concentration of 40 ppm [17]. The electropolymerization of the monomer is depicted in Figure 2.

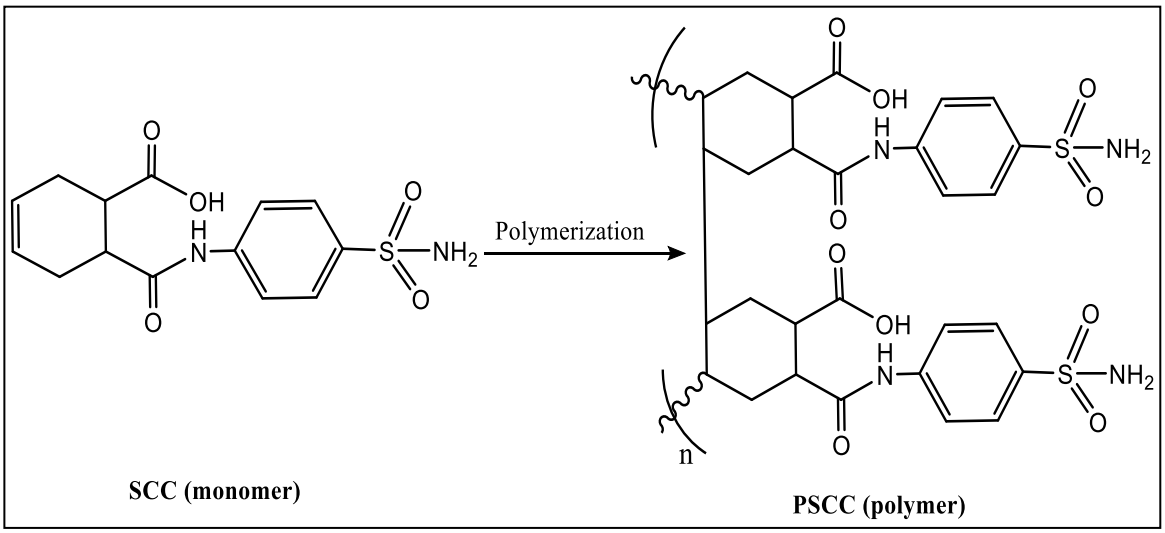

Figure 2: General equation of electropolymerization of SCC monomer.

2.3 Electrochemical Measurements

The electrochemical measurement was performed with Wenking M-lab 200 Electronik Germany Bank potentiostat in a corrosion cell with a double glass wall and three. L.C.S discs act as working electrodes (with a 1 cm^2 surface area); a saturated calomel electrode and a high-purity platinum rod 10 cm long were used as reference and counter electrodes, respectively. These measurements were conducted to assess the corrosion of L.C.S alloy in a salt medium (3.5wt% NaCl) at various temperatures. The solution temperature was controlled using a heating-cooling circulation unit of type HAAKE OOO-3959 from Germany. Polarization curves were captured using a constant sweep rate of 2 mv/s and a scanning range of 200 mv in the negative and positive directions with respect to the open circuit potential. To establish a steady state, the working electrode was immersed in the test cell for fifteen minutes before to starting each experiment.

3. Results & Discussions

3.1 Estimated Mechanism of SCC Monomer Polymerization on L.C.S Electrode Surface

The electrochemical polymerization reactions for grafting and development of the (PSCC) film on the metal surface were characterized by the cationic polymerization mechanism. [18], as shown in scheme 1. The process begins with the transfer of an electron from the monomer to the working electrode (metal surface), resulting in the formation of a radical cation that is generated on the electrode surface, as depicted in steps (1-2). This radical cation may be reacted and then desorbed in the solution to enhance the amount of a component with a low molecular weight. Then, the (SCC) molecule could be added using a cationic mechanism at the charged end of the adsorbed oxidized (SCC) step (3-4).

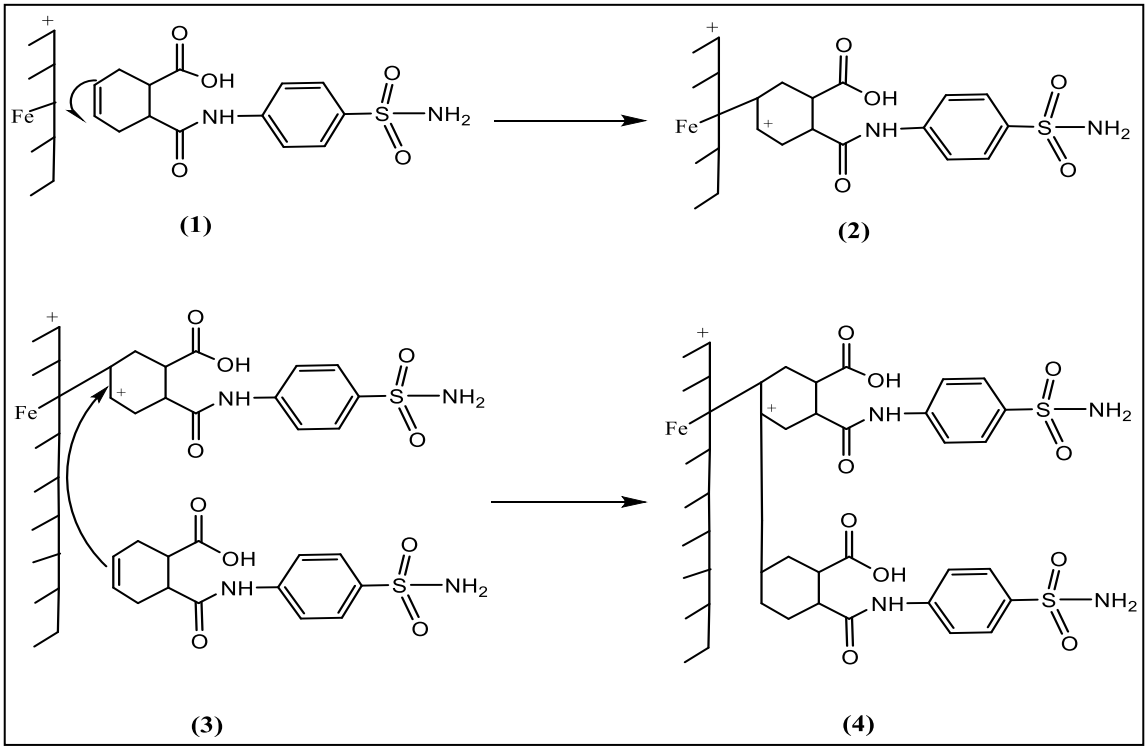

Scheme 1: Supposed Mechanism of Polymerization of SCC on L.C.S electrode.

3.2 Cyclic voltammetry of SCC polymerization on an L.C.S surface

Figure 3 illustrates the first cycle of the voltammogram for a solution of NaCl (3.5%), containing 0.003 M SCC monomer on L.C.S electrode, recorded over a potential range of -200 to +200 mV/SCE at a potential scan rate of 100 mV/s.

The voltammogram showed a very noticeable increase in the anodic current at 1500 mV, indicating the oxidation and polymerization of the SCC monomer to form the polymer coating [19].

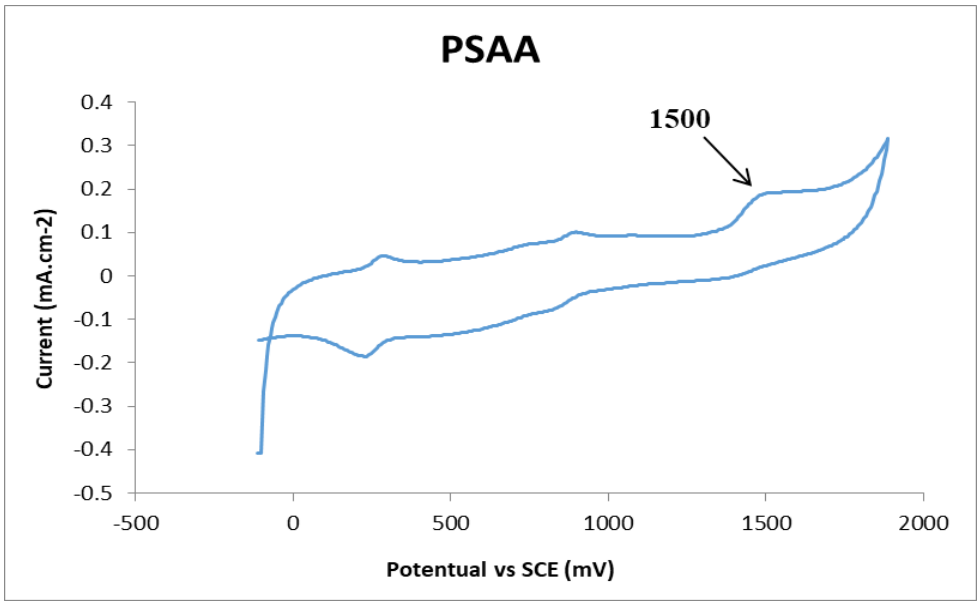

Figure 3: Cyclic voltammogram of PSCC.

3.3 Structural and morphology studies of electropolymerized PSCC films on L.C.S electrode
3.3.1 FTIR spectrum study

As seen in Figure (4), FTIR spectroscopy was employed to analyze the structure of the PSCC polymer, which was synthesized by electropolymerizing the SCC monomer. Figure (4a) shows a stretching band at 3477.42 cm^{-1} for carboxylic OH and the bands at 3350.12 & 3265.26 for the amine group symmetric and asymmetric, respectively, while the band appears at 3114 cm^{-1} for the aromatic C-H and the aliphatic C-H was at 2925.81 and 2856.38 cm^{-1}. The FTIR spectrum showed absorption bands at 1703.03 cm-1 and 1662.52 cm-1, corresponding to the CO acid and CO amide groups, respectively. Additionally, a band at 1595 cm-1 indicated the presence of C=C, and a band at 3033 cm-1 was attributed to olefinic =CH. The FTIR spectrum showed that the C=C bands that appeared in the monomer (SCC) at 1595 cm^{-1} disappeared in the FTIR spectrum of its polymer (PSCC). Also, the disappearance of the olefinic =CH was observed from FTIR spectrum of prepared polymer (Figure (4b)) [20].

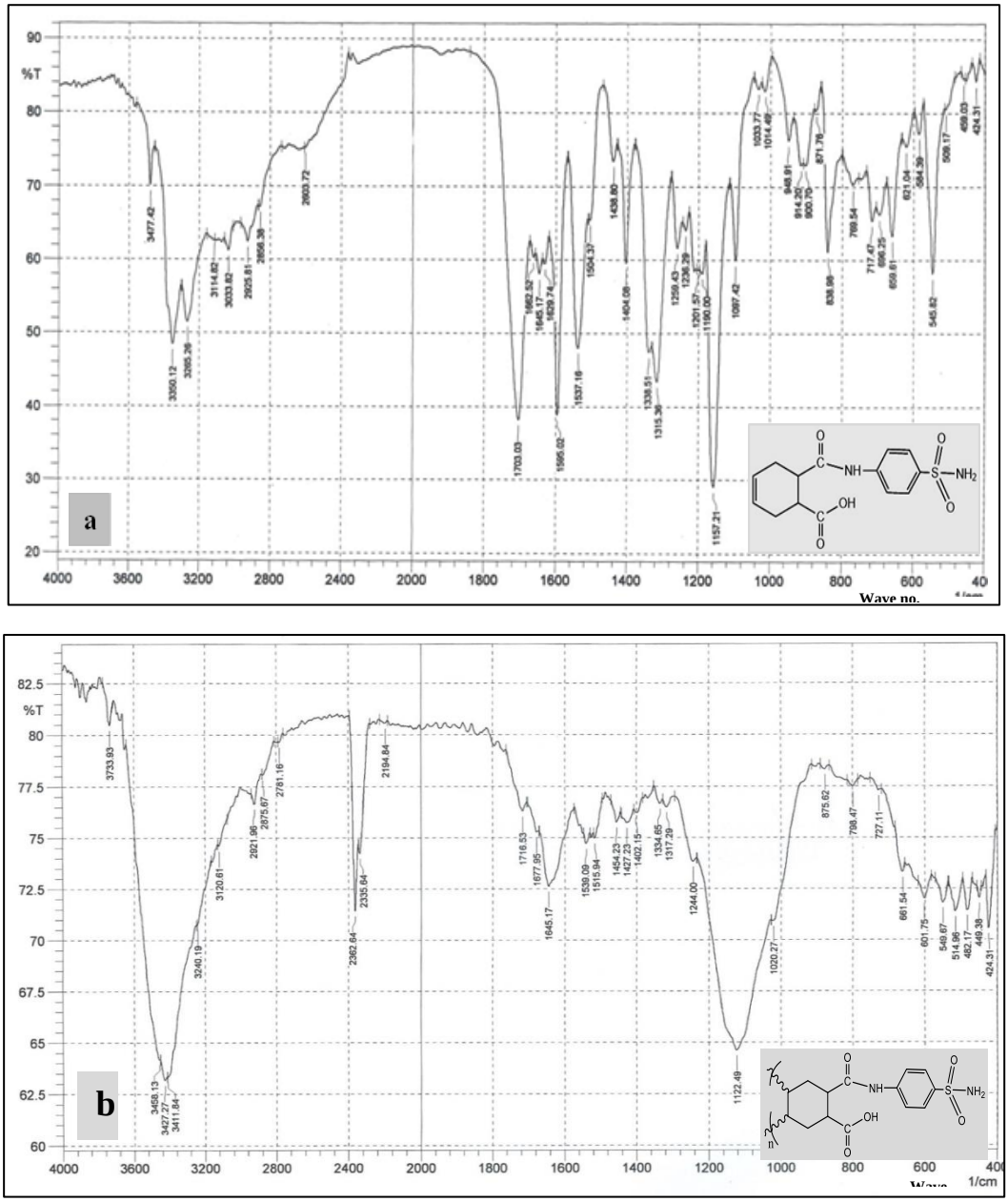

Figure 4: FTIR spectrum of (a) SCC monomer (b) PSCC polymer.

3.3.2 *The surface morphology analysis by AFM and SEM*

A topographical analysis was conducted on the surfaces recorded in 2D and 3D pictures., and root mean square (RMS), average roughness (Ra), and mean diameter for the L.C.S surface coated with polymer and polymer-metal oxides nanocomposite were determined using atomic force microscopy. Table 1 displays the different AFM parameters that were obtained for the L.C.S surface coated with PSCC only and with PSCC-metaloxides nanocomposite.

Figure 5a shows the L.C.S covered solely with PSCC before the addition of nanometal oxides. The surface exhibits an increased roughness average (Ra) value of 203.2 nm, a root mean square (RMS) value of 255.4 nm, and a mean diameter value of 451.9 nm, indicating a high degree of roughness for the polymer-covered L.C.S surface. However, Figure 5b shows the surface of L.C.S covered with PSCC-ZrO_2 nanocomposite; this image depicted a decreased Ra value to 87.02 nm and RMS value of 116.5 nm and a mean diameter value to 83.10 nm, A decreased in RMS infers addition of nanomaterial gives greater homogeneity and smoothness of the polymeric coating and the absence of any corrosion product deposits.
Figure 5c shows the surface of L.C.S covered with PSCC-ZnO nanocomposite; this image showed a decreased Ra value of 59.78 nm, RMS value of 76.87 nm and mean diameter value of 89.91 nm, a decrease in RRMS roughness infers addition of nanomaterial gives greater homogeneity and smoothness of the polymeric coating and the absence of any corrosion product deposits. These results indicate that the nanometal oxides enhanced the PSCC protective film, forming a barrier against attack by aggressive ions from the corrosive environment [21]. Table 1 shows the values of RMS, Ra, and mean diameter for L.C.S covered by PSCC film with and without of the nanomaterials.

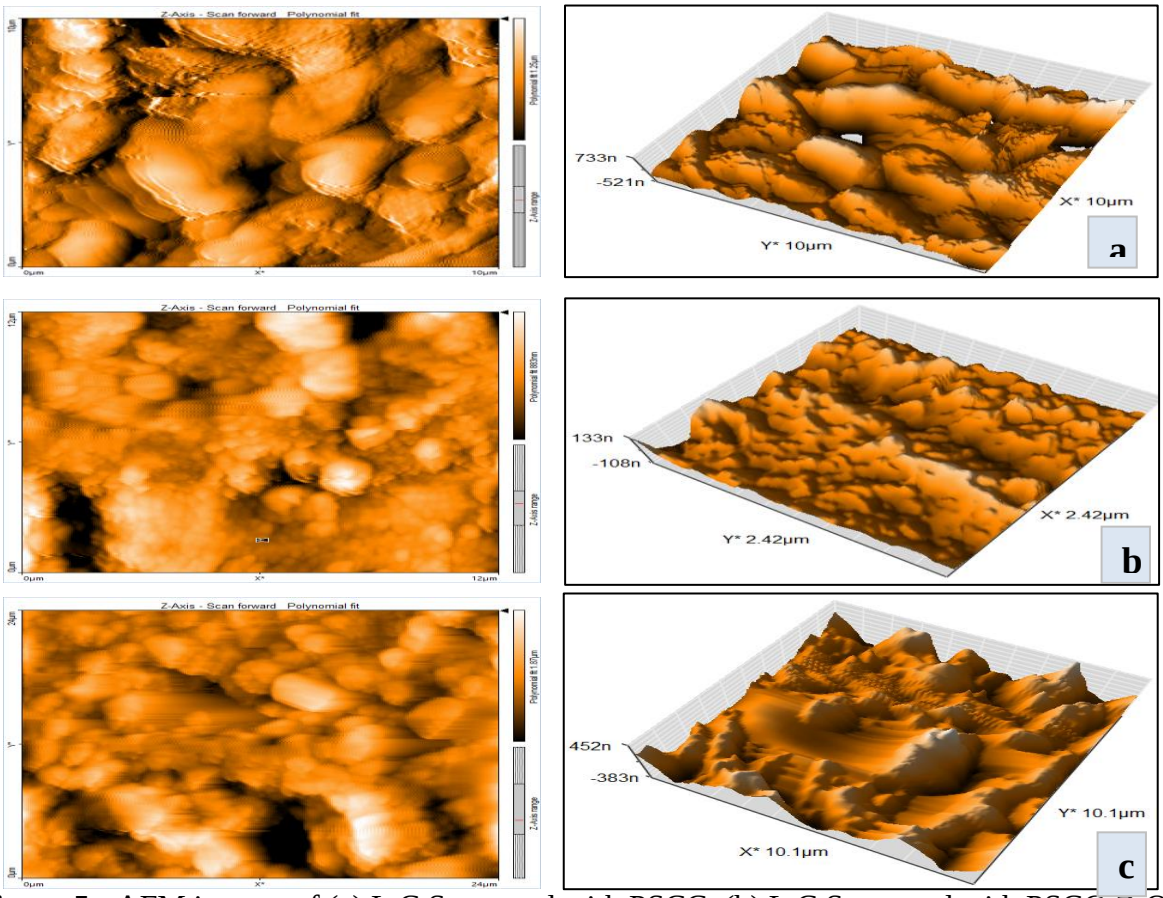

Figure 5 : AFM images of (a) L.C.S covered with PSCC, (b) L.C.S covered with PSCC-ZrO_2 nanocomposite, (c) L.C.S covered with PSCC-ZnO nanocomposite.
Table 1: Surface topography parameters obtained from AFM analysis for L.C.S covered by PSCC filmin the with and without of the nanomaterials.

System	Mean diameter (nm)	RMS (nm)	Ra (nm)
PSCC	451.9	255.4	203.2
PSCC-ZrO_2 nanocomposite	83.10	116.5	87.02
PSCC-ZnO nanocomposite	89.91	76.87	59.78

Scanning electron microscopy (SEM) was used to analyze and compare the surface morphology of the polymer films both with and without the inclusion of nanomaterials. Aggregates diameter was determined to be varied from 198 to 255 nm for pure polymers. The diameter of the polymer's aggregates decreased extremely after adding the nanomaterials, ranging from 15.17 to 19.48 nm. This is indicated the improvement of polymer coatings after modification with nanomaterials, which leads to high corrosion resistance at a scale of 200 nm.

The morphology related to the PSCC polymer (Figure 6a) considerably differs from morphology regarding its nanocomposites (Figures 6b & 6c) in the SEM micrographs, Where the surface of the polymer with no nanometal oxides has brick-like pieces with large pores. Figures (6b& 6c) indicate dense and uniform coatings generated on the surface of L.C.S with homogeneous distributions of the nano ZrO_2 and ZnO dispersed in a matrix of the polymer [22].

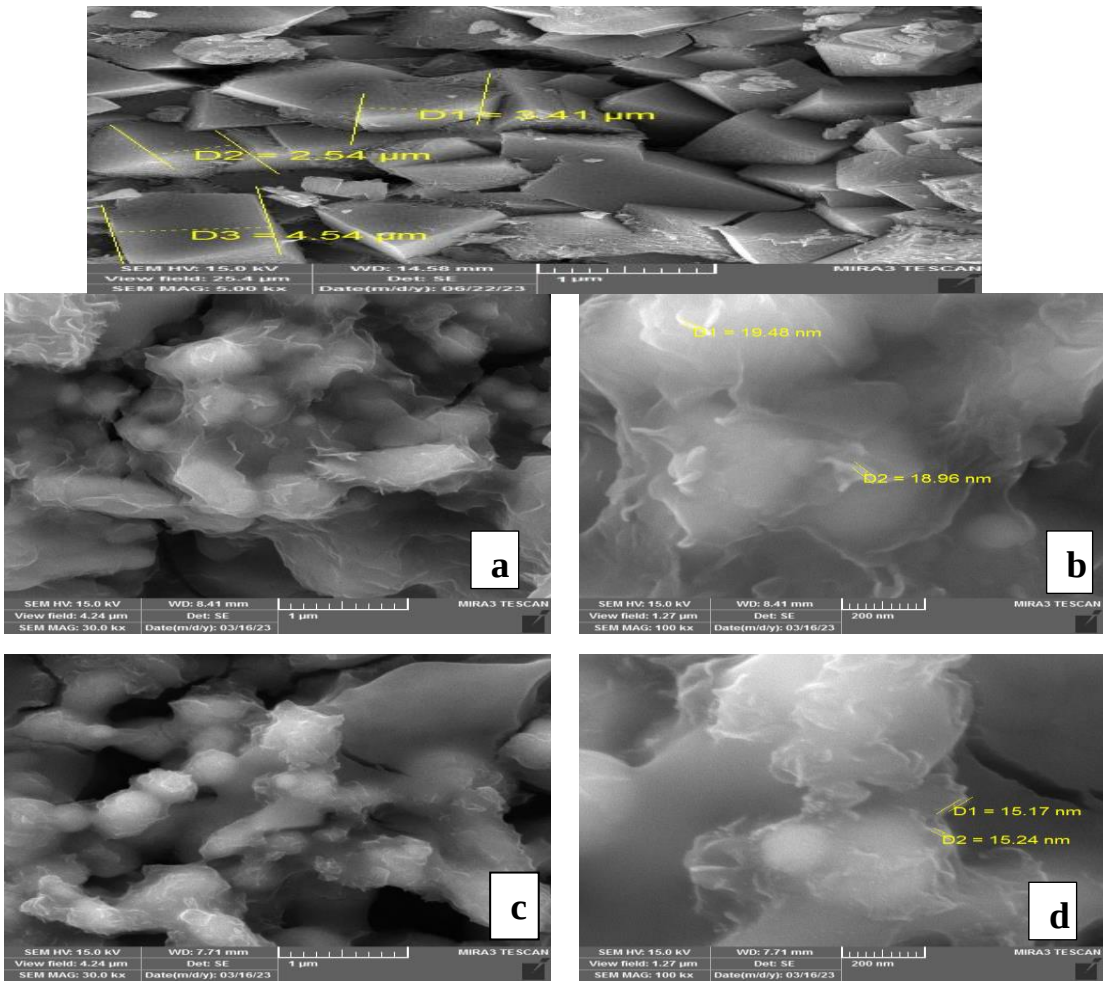

Figure 6: SEM images of (a) L.C.S covered with PSCC, (b) L.C.S covered with PSCC-ZrO_2 nanocomposite, (c) L.C.S covered with PSCC-ZnO nanocomposite

3.4 Corrosion Measurements using Potentiostatic Polarization

The protection properties of the obtained PSCC and PSCC-metaloxides nanocomposite coating were considered in the solution of NaCl (3.5% wt) at different temperatures ranging from (298 to 328)K by a potentiostatic polarization procedure.

Figure 7 presents the polarization curves obtained in the solution of NaCl (3.5% wt) environment for the uncovered L.C.S, the L.C.S covered with PSCC, and the L.C.S covered with the PSCC-metal oxide nanocomposite. These curves were used to calculate the following values: weight loss (WL), penetration loss (PL), cathodic Tafel slope (βa), anodic Tafel slope (βc), corrosion potential (Ecorr), and corrosion current density (icorr) (2). Equation (2) can be used to determine the protection efficiency (PE%) based on the data from the Tafel curves:

$$PE\% = \frac{i_{corr,uncoated} - i_{corr,coated}}{i_{corr,uncoated}} \times 100 \quad \ldots\ldots\ldots (2)$$

Where $i_{corr,\ uncoated}$, $i_{corr,\ coated}$= corrosion current density for uncoated and coated L.C.S respectively. Polarization resistance was also calculated (R_p) using the Stern-Gery equation (Eq. (3)) [23]:

$$R_p = \frac{B_a|B_c|}{2.303(B_a + |B_c|)i_{corr}} \quad \ldots\ldots\ldots\ldots (3)$$

The protective capacity of electrodeposited coatings is assessed using polarization resistance (R_p) measurements since the registered R_p values are inversely proportional to the corrosion current (greater polarization resistance = lower corrosion current). Polarization resistance refers to a material's ability to resist oxidation when an external voltage is applied [24]. In other words, it is a measure of a specimen's resistance to corrosion under polarized conditions. Table 2 presents the values for the specified parameters

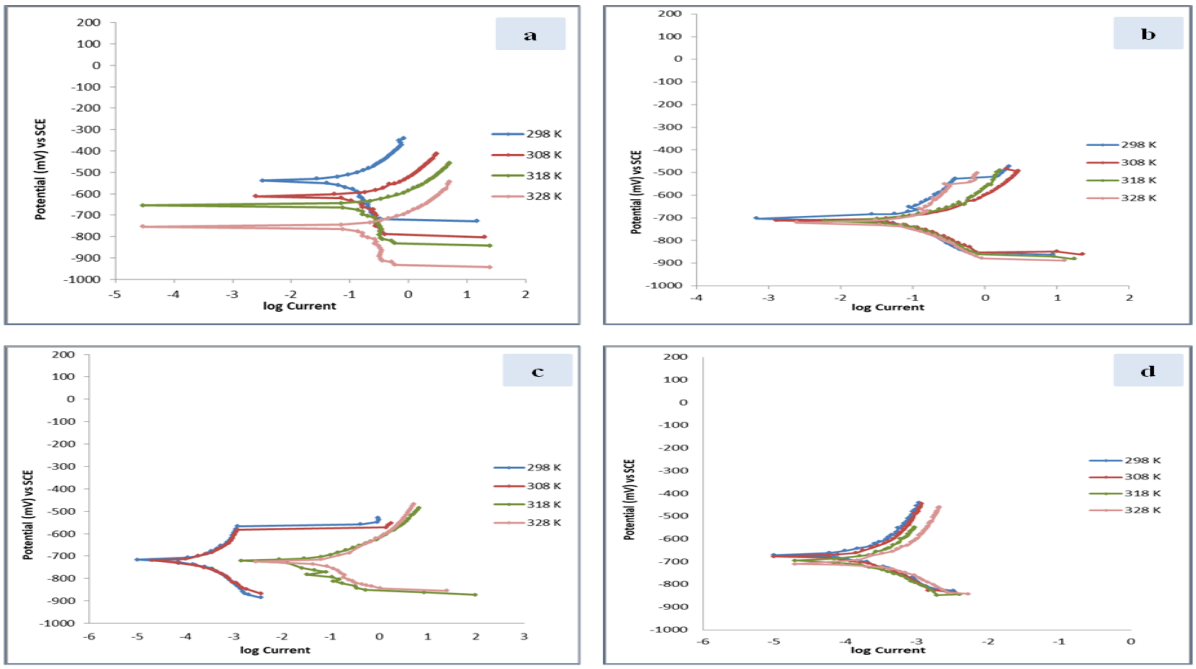

Figure 7: Polarization graphs for (a) uvcovered L.C.S, (b) L.C.S covered with PSCC, (c) L.C.S covered with PSCC-ZrO_2 nanocomposite , (d) L.C.S covered with PSCC–ZnO nanocomposite.

Table 2: Corrosion characteristics of covered and uncovered L.C.S. with PSCC when Nanomaterial-oxides are present and absent in a solution of 3.5% wt NaCl at various temperatures

Material	T (K)	E_{corr} (mV)	i_{corr} (μA/cm^2)	βc (mV/Dec)	βa (mV/Dec)	WL (mm/y)	PL (g/m^2.d)	PE%	R_p (Ω/cm^2)
Uncoated L.C.S	298	-530.0	63.51	-142.1	104.8	1.290	0.593	-	412
	308	-610.0	76.20	-145.1	120.0	1.950	0.900	-	374
	318	-650.0	117.69	-239.4	80.1	2.620	1.220	-	221
	328	691.1	141.82	-449.6	70.9	3.160	1.450	-	187
L.C.S coated with PSCC	298	-703.1	15.52	-68.4	80.6	0.883	0.180	75.56	1035
	308	-711.8	20.17	-68.1	51.4	0.503	0.234	73.53	630
	318	-713.2	33.59	-80.5	75.5	0.840	0.390	71.45	503
	328	-720.5	43.88	-87.4	100.5	1.110	0.509	69.05	462
L.C.S coated with PSCC +ZrO_2 Nanocomposite	298	-716.2	0.20	-152.2	143.9	0.051	0.002	99.67	156358
	308	-718.2	0.28	-250.6	150.0	0.070	0.003	99.62	144750
	318	-720.0	8.28	-62.0	51.7	0.344	0.160	92.96	1478
	328	-725.0	19.41	-66.8	59.0	0.485	0.225	86.31	700
L.C.S coated with PSCC + ZnO Nanocomposite	298	-671.2	0.08	-101.7	132.5	0.021	0.0010	99.86	290507
	308	-678.2	0.15	-138.7	174.5	0.039	0.0018	99.79	215095
	318	-695.5	0.27	-260.1	266.8	0.029	0.003	99.76	183905
	328	-710.0	0.36	-243.1	246.6	0.090	0.004	99.74	147656

Table 2 displays the corrosion characteristics of covered and uncovered L.C.S. with PSCC in a solution of 3.5%wt NaCl in both the existence and free of nanometaloxides temperature range of 298 to 328 K. The results clearly showed that the PSCC polymeric films coated the surface of the L.C.S. alloy, protecting it against corrosion in 3.5% NaCl solution by 75.56% at 298K. Additionally, this data also shown that the addition of ZrO_2 and ZnO NPs to the PSCC and formation PSCC-nanometaloxies nanocomposite L.C.S alloy successfully enhanced the protection efficiency to (99.67 and 99.86 %), respectively.

The R_p values for L.C.S in salt solution (3.5%wt NaCl) without coated with PSCC were low. They decreased with increasing temperature, which is attributed to corrosion product formation (Iron oxides). At the same time, R_p for L.C.S coating with PSCC have higher values than before coating, and the presence of nanometal oxides as also lead to increased R_P values, which means that no corrosion products were formed on L.C.S surface [25].

3.5 Kinetic and thermodynamic activation parameters of corrosion

The temperature can affect L.C.S. corrosion in a 3.5% wt NaCl solution both in the presence and absence of coating. Potentiostatic tests are made at different temperatures (298 to 328 K) with and withiut of PSCC and PSCC-metal oxides nanocomposite to evaluate the corrosion process's activation energy. Table 3 displays the relevant results. The Arrhenius equations (Eq. (4, 5)) were employed to determine the formation of the activated complex in the transition state, allowing for the calculation of the activation parameters associated with the corrosion process [26].

$$\log C.R = \log A - \frac{E_a}{2.303\ RT} \quad \ldots\ldots\ldots(4)$$

$$\log \frac{C.R}{T} = \log\left(\frac{R}{Nh}\right) + \frac{\Delta S^*}{2.303\ R} - \frac{\Delta H^*}{2.303RT} \quad \ldots\ldots\ldots(5)$$

Where C.R = the corrosion rate that is equivalent to the corrosion current, E_a= the apparent effective activation energy, R= the molar gas ($JK^{-1}mol^{-1}$) constant, A= the Arrhenius preexponential factor, and T= the absolute temperature (K), N= Avogadro's number, h= Planck constant.

Conversely, the activation free energy values' value ΔG^* is estimated utilizing Gibbs equation (Eq. (6)).

$$\Delta G^* = \Delta H^* - T\Delta H^* \quad \ldots\ldots\ldots\ldots(6)$$

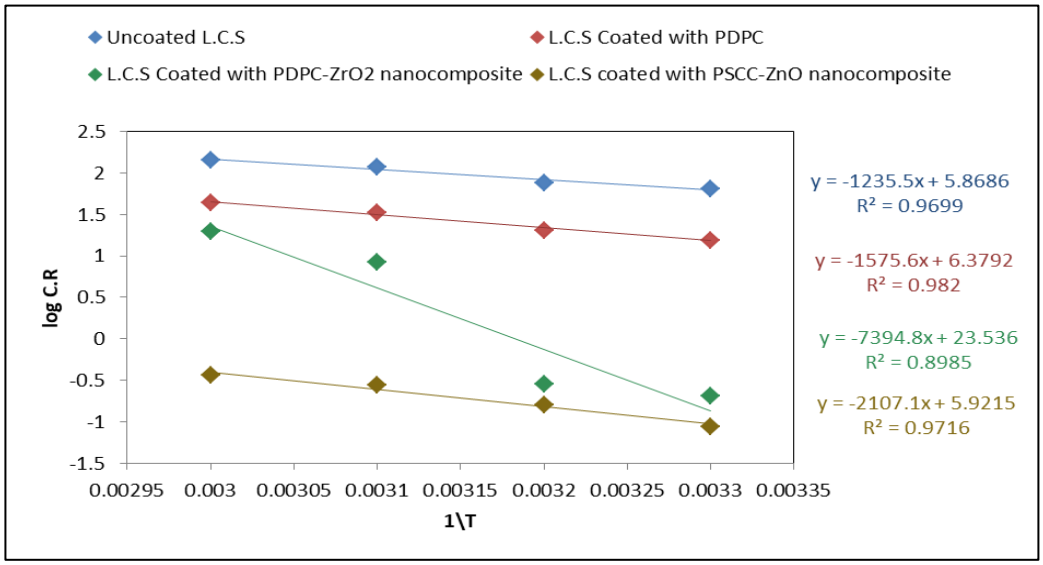

Figure 8: The relation between log C.R & (1\T) for uncovered L.C.S and PSCC-covered L.C.S. with and without nanomaterial oxides in 3.5% wt NaCl solution

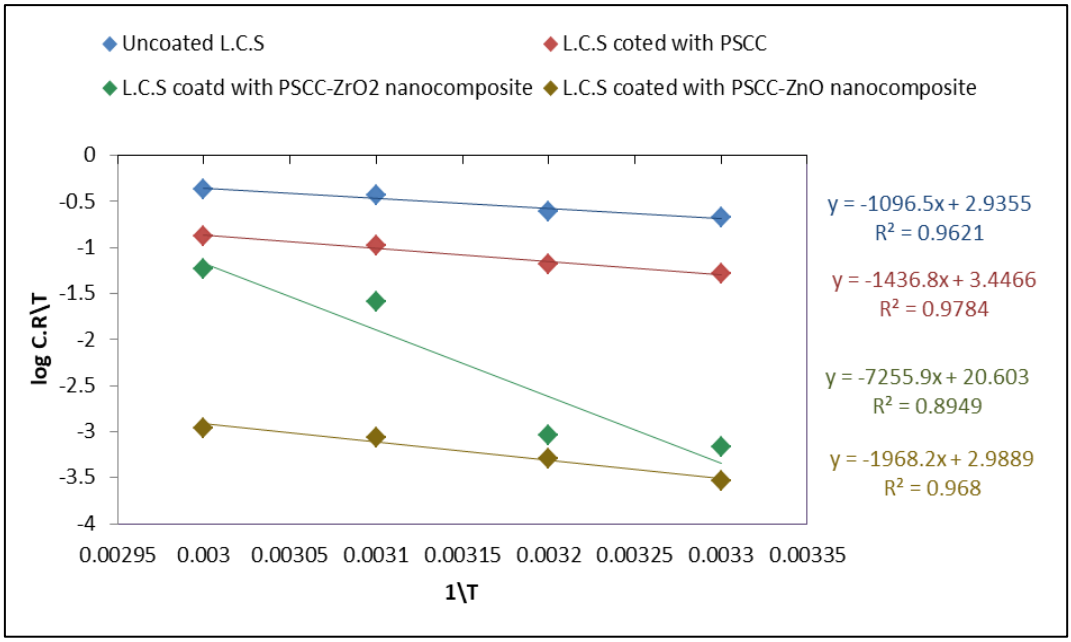

Figure 9: The relation between log (C.R/T.) and (1T) for uncovered L.C.S. and PSCC-covered L.C.S. with and without nanometal oxides in 3.5% wt NaCl solution.

Table 3: Transition state thermodynamic and kinetic parameters at different temperatures for the corrosion of uncovered L.C.S. and PSCC-covered L.C.S. with and without nanomaterial oxides in 3.5% NaCl solution

System	T	ΔG^* (kJ)	E_a^* (kJ\mol)	A (Molecule .cm^{-2}. S^{-1})	ΔH^* (kJ\mol)	ΔS^* (J/mol. K)
Uncovered L.C.S	298	63.123	23.656	4.448×10^{29}	20.994	-141.373
	308	64.536				
	318	65.950				
	328	67.364				
L.C.S covered with PSCC	298	66.722	30.168	1.441×10^{30}	27.510	-131.587
	308	68.038				
	318	69.354				
	328	70.670				
L.C.S covered with PSCC-ZrO_2 nanocomposite	298	81.251	141.589	2.068×10^{47}	138.929	196.908
	308	78.282				
	318	76.313				
	328	74.344				
L.C.S covered with PSCC-ZnO nanocomposite	298	79.509	40.344	5.024×10^{29}	37.685	-140.351
	308	80.913				
	318	82.316				
	328	83.720				

Figure 8: illustrates how the activation energy (Ea) and the Arrhenius preexponential factor (A) were determined by a linear regression between log C.R and 1/T. According to the current study, the value of A is greater when PSCC and PSCC-metal oxide nanocomposite are present than when they are not.

The activation energy values increased with the addition of different nanometal oxides in the coatings. This indicates that the energy barriers for the corrosion reaction were enhanced, making it more difficult for the corrosion process to occur. indicating a strong protective action of PSCC and PSCC-metal oxides nanocomposite by increasing the energy barrier of reaction of corrosion [27].

Lines that are straight with an intercept of [log (R/Nh)+(ΔS*/2.303R)] and a slope of (ΔH*/2.303R). were obtained by the use of plots (Figure 9) that illustrate the relationship between the reciprocal of absolute temperature (1/T) and log (C.R/T). From these plots, the values of ΔH* and ΔS*, respectively, were computed and included in Table 3. The endothermic nature of the L.C.S dissolution process is indicated by the positive values of ΔH* in both the coating layer's presence and absence. Table 3 further illustrates how the activation enthalpy

and activation energy values varied in a similar way. This outcome confirmed the established thermodynamic relationship between Ea and ΔH* [28, 29]. The activation complex in the rate-determining step appears to represent an association rather than a dissociation step, indicating that there is an increase in disordering during the transition from reactants to the activated complex, according to the increases in the activation entropy values in the presence of the coating layer. Table 3 shows that the free activation energy has positive values. Additionally, very little change was seen as the temperature increased, suggesting that the activated complexes were unstable and that the probability of their creation was lowered. [30].

4. Conclusion

Polymeric films (PSCC) were prepared on the surface of L.C.S by electropolymerization of the monomer (SCC). It was observed that the double bond (C=C) disappeared in the FTIR spectrum of the polymer despite its presence in the FTIR spectrum of the monomer. In a saline media (3.5% NaCl), the produced polymeric films (PSCC) offer good protection for the L.C.S alloy surface against corrosion; however, the effectiveness of this protection declines with temperature. By adding nanomaterial oxides like ZrO_2 and ZnO, the produced polymeric films' ability to shield the L.C.S. from corrosion is increased. The kinetic and thermodynamic analysis demonstrated that the rising energy barrier for the corrosion process caused the activation energies of L.C.S. corrosion to rise following coating. The addition of various nanomaterials results in higher activation energy values, and coatings raise the corrosion reaction's energy barriers. The endothermic nature of transition state processes is indicated by the positive values of activation enthalpy (ΔH*) for both coated and uncoated L.C.S. metallic surface. Lastly, AFM and SEM studies demonstrated that L.C.S. was protected because protective coatings were created on the metal surface, which had stronger barrier effects.

5. Acknowledgement

Sincere gratitude is extended by the authors of this study to the College of Science's presidency and Chemistry Department staff for providing the facilities needed to finish this work.

References

[1] B. Yao, G. Wang, J. Ye and X. Li, "Corrosion inhibition of carbon steel by polyaniline nanofibers, " *Materials Letters*, vol. 62, pp. 1775–1778, 2008.

[2] A. Alsamuraee, H. Jaafer, H. Ameen and A. Abdullah," Electrochemical impedance spectroscopic evaluation of corrosion protection properties of polyurethane /polyvinyl chloride blend coatings on steel," *American Journal of Science and Indesterial Res*earch, vol. 2, no. 5, pp. 761-768, 2011.

[3] S. Harsimran, K. Santosh and K. Rakesh, "Overview of corrosion and its control: A critical review, "*Proceedings on Engineering Sciences*, vol. 03, no. 1, pp. 13-24, 2021.

[4] A. Prabhu, V. Venkatesha, V. Shanbhag, M. Kulkarni and G. Kalkhambkar, "Inhibition Effects of Some Schiff's Bases on the Corrosion of Mild Steel in Hydrochloric Acid Solution,"*Corrosion Science*, vol. 50, pp. 3356-3362, 2008.

[5] L. Han and S. Song, "A Measurement System Based on Electrochemical Frequency Modulation Technique for Monitoring the Early Corrosion of Mild Steel in Seawater," *Corrosion Science*, vol. 50, pp. 1551-1557, 2008.

[6] H. Recio, P. Ocon and E. Fatás, "Effect of the polymer layers and bilayers on the corrosion behaviour of mild steel: Comparison with polymers containing Zn microparticles", *Progress in Organic Coatings*, vol. 54, no. 4, pp. 285-291, 2005.

[7] A. Kumar, "Role of conducting polymers in corrosion protection," *World Journal of Advanced Research and Reviews*, vol. 17, no. 02, pp. 045–047, 2023.

[8] S. Sriwichai, P. Netsuwan, S. Phanichphant, and A. Baba, "Electropolymerization and Properties of Poly (3-anilinethiophene) Thin Film," *Chiang Mai Journal of Science*, vol. 43, no. 4, pp. 863-869, 2016.

[9] C. Nascentes, I. Aguilar, G. Gil-Ramírez, and J. Gonzalez-Rodriguez, "Electropolymerization of Metallo-Octaethylporphyrins: A Study to Explore Their Sensing Capabilities," *Materials*, vol. 15, no.19, 2022.

[10] H. Shokry, "Corrosion protection of mild steel electrode by electrochemical polymerization of acrylamide," *Chemistry of Metals and Alloys*, vol. 2, pp. 202-210, 2009.

[11] H. Xu and Y. Zhang, "A Review on Conducting Polymers and Nanopolymer Composite Coatings for Steel Corrosion Protection", *Coatings*, vol. 9, no. 807, 2019.

[12] K. Sharma, M. Goyat and P. Vishwakarma, "Synthesis of Polymer Nanocomposite coatings as corrosion inhibitors: A quick review," *IOP Conf. Series: Materials Science and Engineering*, vol. 983, no. 012016, 2020.

[13] 13. I. Shakir, A. Alsamurraee and S. Saleh, "Pitting Corrosion Behavior of 304 SS and 316 SS Alloys in Aqueous Chloride and Bromide Solutions," *Journal of Engineering*, vol. 24, no. 1, 2018.

[14] 14. S. Habeeb, M. Ali, "study the efficiency of poly nicotine amide as anticorrosion coating on stainless steel and study its biological activity," *Ibn Al-Haitham Journal for Pure and Applied Sciences*, vol. 35, no. 4, 2022.

[15] 15. M. Ali and K. Saleh, "corrosion protection studies of stainless steel alloy in hydrochloric acid by using electropolmerized poly (N-imidazoly tetrahydrophthalamic acid)," *International journal of engineering and technology*, vol. 7, no. 4, 2018.

[16] 16. A. Al-qudsi and K. Saleh, "electrochemical polymerization of eugenol and corrosion protection studies of stainless steel 304L alloy, " *Journal of medicinal and chemical sciences*, vol. 6, no. 2023, 2023.

[17] 17. M. G. Hosseini, R. Bagheri, R. Najjar, "Electropolymerization of Polypyrrole and Polypyrrole-ZnO Nanocomposites on Mild Steel and Its Corrosion Protection Performance," *Journal of Applied Polymer Science*, vol. 121, pp. 3159–3166, 2011.

[18] 18. E. Younang et al., "Prospective theoretical and experimental study towards electrochemically grafted poly (N-vinyl-2-pyrrolidone) films on metallic surfaces" *Molecular Engineering*, vol. 1, no. 4, pp. 317-332, 1992.

[19] 19. S. El Aggadi, N. Loudiyi, A. Chadil, E. Zoubida and A. El Hourch, "Electropolymerization of aniline monomer and effects of synthesis conditions on the characteristics of synthesized polyaniline thin films," *Mediterranean Journal of Chemistry*, vol. 10, no. 2, pp. 138-145, 2020.

[20] 20. M. Silverstein, X. Webster and J. Kiemle, "Spectrometric Identification of Organic Compounds," 7th ed., *John Wiley & Sons*, Westford, US, 1963.

[21] 21. R. Sudhakaran, C. Thangavelu, M. Sekar, T. Kasilingam and T. Asokan, "Surface analysis of mild steel protected from corrosion by a binary inhibitor formulation containing Zn^{2+} and citrate," *International Journal of Scientific & Engineering Research*, vol. 7, no. 8, 2016.

[22] 22. M. Mobin, J. Aslam, and R. Alam, "Corrosion protection of poly (aniline-co-N-ethylaniline)/ZnO nanocomposite coating on mild steel," *Arabian Journal for Science and Engineering*, vol. 42, no. 1, pp. 209-224, 2017.

[23] 23. M. Lorenzetti, E. Pellicer, J. Sort, M.D. Baró, J. Kovač, S. Novak, and S. Kobe, "Improvement to the corrosion resistance of Ti-based implants using hydrothermally synthesized nanostructured anatase coatings, " *Materials*, vol 7, no. 1, pp. 180-194, 2014.

[24] 24.Y. Toshev, V. Mandova, N. Boshkov, D. Stoychev, P. Petrov, N. Tsvetkova, G. Raichevski, C h. Tsvetanov, A. Gabev, R. Velev and K. Kostadinov, "Protective coating of zinc and zinc alloys for industrial applications," *4M 2006 - Second International Conference on Multi-Material Micro Manufacture ,elsevier*, pp. 323-326, 2006.

[25] 25. N. Khudhair and A. Al-Sammarraie, "Enhancing of Corrosion Protection of Steel Rebar in Concrete Using TiO_2 Nanoparticles as Additive," *Iraqi Journal of Science*, vol. 60, no. 9, pp 1898-1903, 2019.

[26] 26. A. Al-Sammarraie and M. Raheema, "Reduced Graphene Oxide Coating for Corrosion Protection Enhancement of Carbon Steel in Sea water," *Iraqi Journal of Science*, Special Issue , Part B, pp. 243-250, 2016.

[27] 27. M. Solomon, A. Umoren, I. Udosoro and P. Udoh, "Inhibitive and adsorption behaviour of carboxymethyl cellulose on mild steel corrosion in sulphuric acid solution," *Corrosion Science*, vol. 52, no. 4, pp. 1317-1325, 2010.

[28] 28. F. Bentiss, M. Bouanis, B. Mernari, M. Traisnel, H. Vezin and M. Lagrenee, "Understanding the adsorption of 4H-1,2,4-triazole derivatives on mild steel surface in molar hydrochloric acid," *Applied Surface Science*, vol. 253, no.7, PP. 3696-3704, 2007.

[29] 29. Z. Hussain, Z. Fadhil, S. Kareem, S. Mohammed, and E. Yousif, "Removal of organic contaminants from textile wastewater by adsorption on natural biosorbent," *Materials science forum*, vol. 1002, pp. 489-497, 2020.

[30] 30. G. Avci, "Materials science forum Corrosion inhibition of indole-3-acetic acid on mild steel in 0.5 M HCl, " *Colloids and Surfaces A: Physicochemical and Engineering Aspects*, vol. 317, no. 1-3, pp. 730-736, 2008.